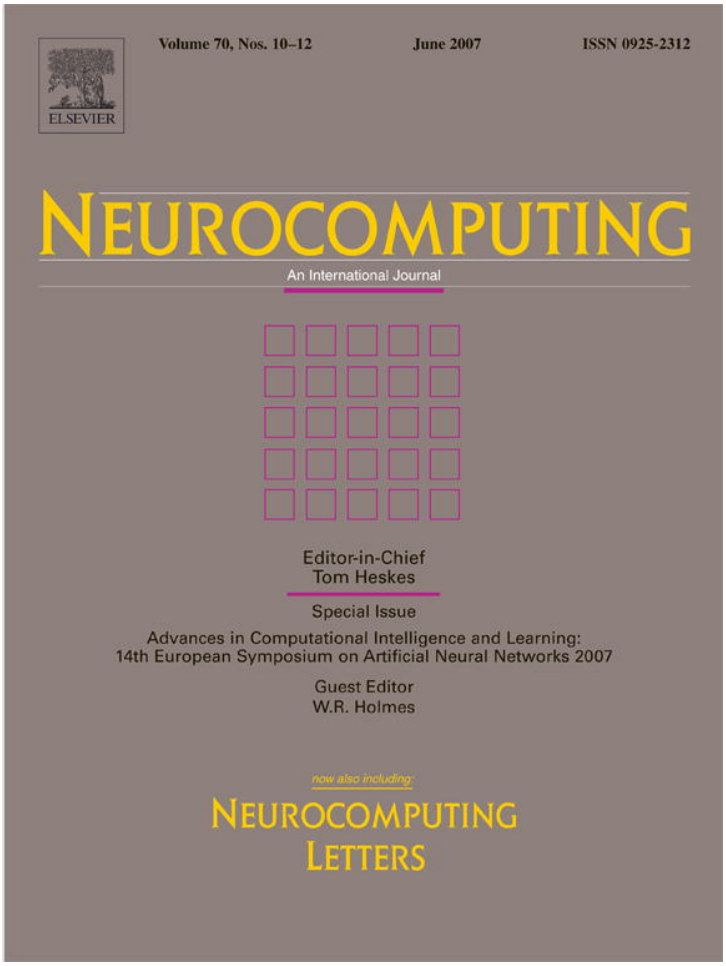

Available online at www.sciencedirect.com
ScienceDirect
Neurocomputing 70 (2007) 1741–1747
NEUROCOMPUTING
www.elsevier.com/locate/neucom

Simple conditions for forming triangular grids

Bálint Takács, András Lőrincz*

Eötvös Loránd University, Budapest, Pázmány Péter sétány 1/C, H-1117, Hungary

Available online 14 November 2006

Abstract

We have used simple learning rules to study how firing maps containing triangular grids—as found in in vivo experiments—can be developed by Hebbian means in realistic robotic simulations. We started from typical non-local postrhinal neuronal responses. We found that anti-Hebbian weight pruning can develop triangular grids under certain conditions. Experimental evidences and the present study suggest that within this model, whitening is a bottom-up process, whereas weight pruning and possibly the non-linear extension of whitening to bottom-up information maximization are guided by top-down influences that reorganize entorhinal responses. We connect our model to the computational model of the entorhinal–hippocampal region of Lőrincz and Buzsáki. In the joined model, the hippocampus is the origin of response reorganization. The joined model may provide insights for memory reorganization guided by hippocampal supervision.

Keywords: Hippocampus; Entorhinal cortex; Triangular grid; Comparator model

1. Introduction

Our study concerns receptive field formation at the superficial layers of the entorhinal cortex (EC). Experimental findings show that responses of neurons in the medial entorhinal cortex (MEC) form triangular grids [6,7]. According to these studies, grid spacing may differ for different neurons and non-grid like activity maps are present at other locations, e.g., at the postrhinal–entorhinal border. Further, the triangular structure in the superficial layers is corrupted if the hippocampus (HC) is lesioned. These findings motivate our studies, because ample clinical and experimental evidence is available to support the view that the hippocampal formation is essential for the alteration of synaptic connections in those cortical networks whose activity gave rise to hippocampal input [12–14] and because the superficial layers of the EC are among these structures and are the closest to the HC.

We have investigated the conditions that may give rise to triangular grids formation subject to Hebbian-like learning in realistic robotic simulations. Our findings are detailed here. The paper is constructed as follows. Section 2 is about the details of our robotic simulations. It also describes the methods that we applied in our numerical studies. Section 3 contains our findings. In the discussion section (Section 4) we interpret the results. We also show that our results fit the computational model of the entorhinal–hippocampal region of Lőrincz and Buzsáki and extend the previous interpretation by connecting the two models. Conclusions are drawn in the last section (Section 5).

2. Methods

2.1. The robot

The open source Khepera simulator[1] was used. The robot was 'placed' in a circular 'labyrinth'. The robot had a diameter of 55 mm. The radius of the circle was 200 mm. Sensory information included '*whiskers*', the wide angle infrared proximity sensors of Khepera, '*peripheral motion detectors*', the angular speed of the wheels, and '*visual information*' the 16 pixel activities of the linear pixel array camera (the turret) of Khepera as well as several—typically

*Corresponding author. Tel.: +36 209 0555/8473.
E-mail addresses: takbal@elte.hu (B. Takács), andras.lorincz@elte.hu (A. Lőrincz).

[1]YAKS simulator: http://yaks.ida.his.se/.

0925-2312/$ - see front matter © 2006 Elsevier B.V. All rights reserved.
doi:10.1016/j.neucom.2006.10.127

26—'*invariant detectors*'. The detection range of the infrared sensors is about 40 mm.

The vision turret had a range of 300 mm with a field-of-view of 270° split evenly by 16 sensors. Cues were put onto the wall at 60°, the width of the cues was 5 mm. The output of a visual sensor was 1 if a cue was within range in its direction, otherwise the output decreased linearly from 0.5 (0 mm) to 0 (300 mm) as a function of the distance of the robot from the wall in the sensor's increased. Visual inputs were affected by a small noise. Typical activities are shown in Fig. 1(a) as a function of time.

Invariant detectors were formed by mixing randomly chosen Gaussian blobs out of a pool of 1000 blobs. Blob positions were chosen randomly in the environment. Blob sizes were also random, they were drawn from a finite, but not too broad range that we varied. Blobs for each invariant sensor were drawn randomly with 2% probability from the pool of blobs. Typical activity maps are shown in Fig. 1(b). These invariant detectors can be considered as outputs of neurons that process sensory information.[2] In fact, these invariant responses *are similar* to those found in the postrhinal cortex, the main input source of the MEC [6].

The robot was equipped with a simple controller, which preferred to move forward with occasional random changes of the direction and turned away when the short-range infrared detectors sensed the wall.

The outputs of the detectors made the input of the learning system without any information about the nature of the sensors and about the relative topography, e.g. the neighboring relations between the visual sensors.

2.2. Learning rules

We have trained the putative afferents of superficial layers of the EC by using the outputs of our 'sensors' and by means of different Hebbian learning rules. We have tried, among others, the following *on-line* learning rules and their combinations: (i) anti-Hebbian weight pruning rule (Eq. (1)), (ii) whitening (Eq. (2)), and (iii) *infomax* learning rule for independent component analysis (ICA) (Eq. (3)) as well as the combinations: (iv) whitening and weight pruning (Eq. (4)) and (v) ICA and weight pruning (Eq. (5)):

$$\Delta \mathbf{W} = -\alpha \mathbf{y}\mathbf{x}^{\mathrm{T}}, \tag{1}$$

$$\Delta \mathbf{W} = \beta(\mathbf{I} - \mathbf{y}\mathbf{y}^{\mathrm{T}})\mathbf{W}, \tag{2}$$

$$\Delta \mathbf{W} = \beta(\mathbf{I} - f(\mathbf{y})\mathbf{y}^{\mathrm{T}})\mathbf{W}, \tag{3}$$

$$\Delta \mathbf{W} = -\alpha \mathbf{y}\mathbf{x}^{\mathrm{T}} + \beta(\mathbf{I} - \mathbf{y}\mathbf{y}^{\mathrm{T}})\mathbf{W}, \tag{4}$$

$$\Delta \mathbf{W} = -\alpha \mathbf{y}\mathbf{x}^{\mathrm{T}} + \beta(\mathbf{I} - f(\mathbf{y})\mathbf{y}^{\mathrm{T}})\mathbf{W}, \tag{5}$$

where α, β are positive constants, $\mathbf{x} \in \mathbb{R}^n$ and $\mathbf{W} \in \mathbb{R}^{m \times n}$ denote the input vector and the transformation to be learned, respectively, superscript T denotes transposition, $\mathbf{y} \in \mathbb{R}^m$ is the output vector of the trained neurons, n took different values for different sensory systems, m, i.e., the number of neurons was 26, nonlinearity $f(.)$ was the tanh(.) function.

[2]We shall refer to detector outputs both as the sensory information (of the robot) and as the responses of neurons (that provide bottom-up input to the superficial layers of the EC).

2.3. Computing triangular grid statistics

The pseudocode of the algorithm is as follows:

(1) Compute

$$C_I(x,y) = \sum_{\Delta x} \sum_{\Delta y} I(x,y) I(x+\Delta x, y+\Delta y),$$

the 2D cross-correlogram of the activity map $I(x,y)$, where x and y denote the two dimensional coordinates, I is the average output of one of the neurons at point (x,y), i.e., I is a shorthand for one of the coordinates of vector $\mathbf{y}$.

(2) Normalize the correlogram at each point: Let

$$C'_I(x,y) = C_I(x,y)/C_M(x,y),$$

where $C_M(x,y)$ is the binary mask for $I(x,y)$.

(3) Find all local maxima $M_i(x_i, y_i)$ in the normalized correlogram $C'_I(x,y)$.

(4) Join those peaks which are too close:
   (a) Calculate the distances $d(i,j)$ for all peaks,
   (b) find the smallest $d(k,l)$ and finish if $d(k,l) > 3$ pixels, otherwise
   (c) substitute $x_k := (x_k + x_l)/2$ and $y_k := (y_k + y_l)/2$ and delete M_l from the list of maxima, then start over from calculating all the distances.

(5) Compute the Delaunay-triangularization of the M_i peaks. Leave out those edges that do not belong to 2 triangles to remove the edges on the boundary.

3. Results

We could barely detect triangular grids when the Khepera's original sensory information was used, because of the direction dependence of these sensors. We could emerge triangular grids only when we used the invariant detectors. Even in this case, receptive field formation by whitening provided ordered structures but not grids (Fig. 2(a)). Whitening and weight pruning together could develop triangular grids for certain α and β parameter regions of Eq. (4) (Fig. 2(b)). ICA alone did not develop triangular grids either, but resulted in place cells (Fig. 2(c)). However, ICA and weight pruning together produced triangular grids. In this case, i.e., for ICA and weight pruning, grid formation occurred in a somewhat broader parameter range than for weight pruning combined with

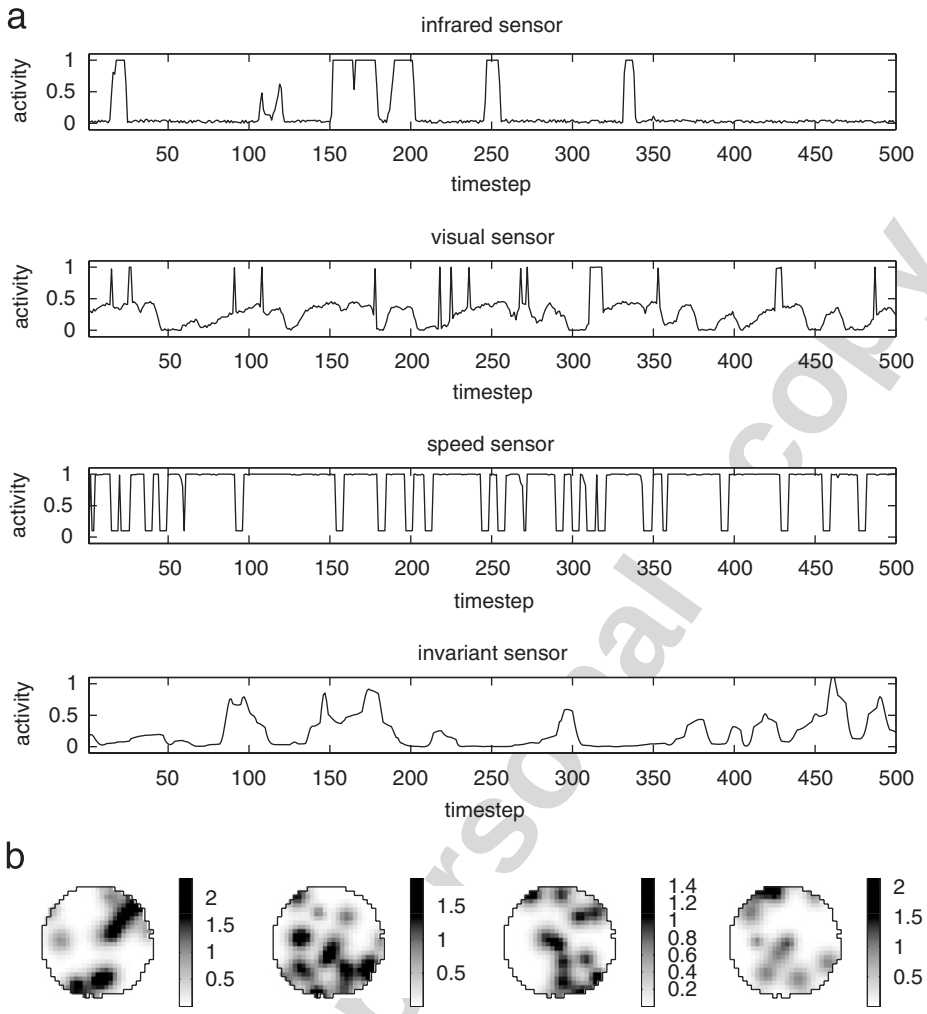

Fig. 1. *Sensory responses*: Invariant sensors were generated as follows. To each invariant receptive field Gaussian blobs were drawn randomly with 2% probability from a pool of 1000 randomly generated Gaussian blobs. The average number of Gaussian blobs within invariant receptive fields is about 20. (a) Examples of responses of infrared, visual, speed and invariant sensors versus time in the circular labyrinth. (b) Examples of invariant sensor activity maps.

whitening. Also, grid formation was more robust in this case. Grid formation as a function of training time using ICA and weight pruning is depicted in Fig. 2(d).

Another finding concerns grid spacings. Recall that invariant sensors were generated by mixing blobs. The average size of the blobs influenced grid spacing: larger average blob sizes give rise to larger grid spacing. Thus, our model enables the emergence of neural responses that represent triangular grids, the spacing of these grids may differ for different neurons and non-grid like responses emerge if inputs have strong direction dependence.

4. Discussion

First we summarize our results and then we build up our conjectures. We shall relate our model to a computational model of the entorhinal–hippocampal loop [10]. Finally, we comment on recent attractor models of triangular grid formation in the superficial layers of the EC [16,5].

We could form triangular grids by assuming rotation invariant neural responses, similar to the approximately invariant neural responses in the postrhinal cortex. However, neither whitening nor ICA, the widely accepted learning candidates for bottom-up processing transformations [1,2] could produce grid like activity maps. Moreover, ICA produced *place cells* from the same invariant neuronal responses. These findings are intriguing, because place cells are formed at the HC and not at the EC and thus, if we use only linear transformations (i.e., matrix **W** in Eqs. (1)–(5)) without loss of information to form superficial responses, then it would be warranted that ICA, the putative function of the HC in the computational model [9,10], will form place cells from the entorhinal inputs under all conditions. In other words, if we can form triangular grids by Hebbian tuning of linear transformations, then the model can be connected to previous functional models of the EC–HC loop.

We have tried several learning methods to form triangular grids. We succeeded by anti-Hebbian like weight

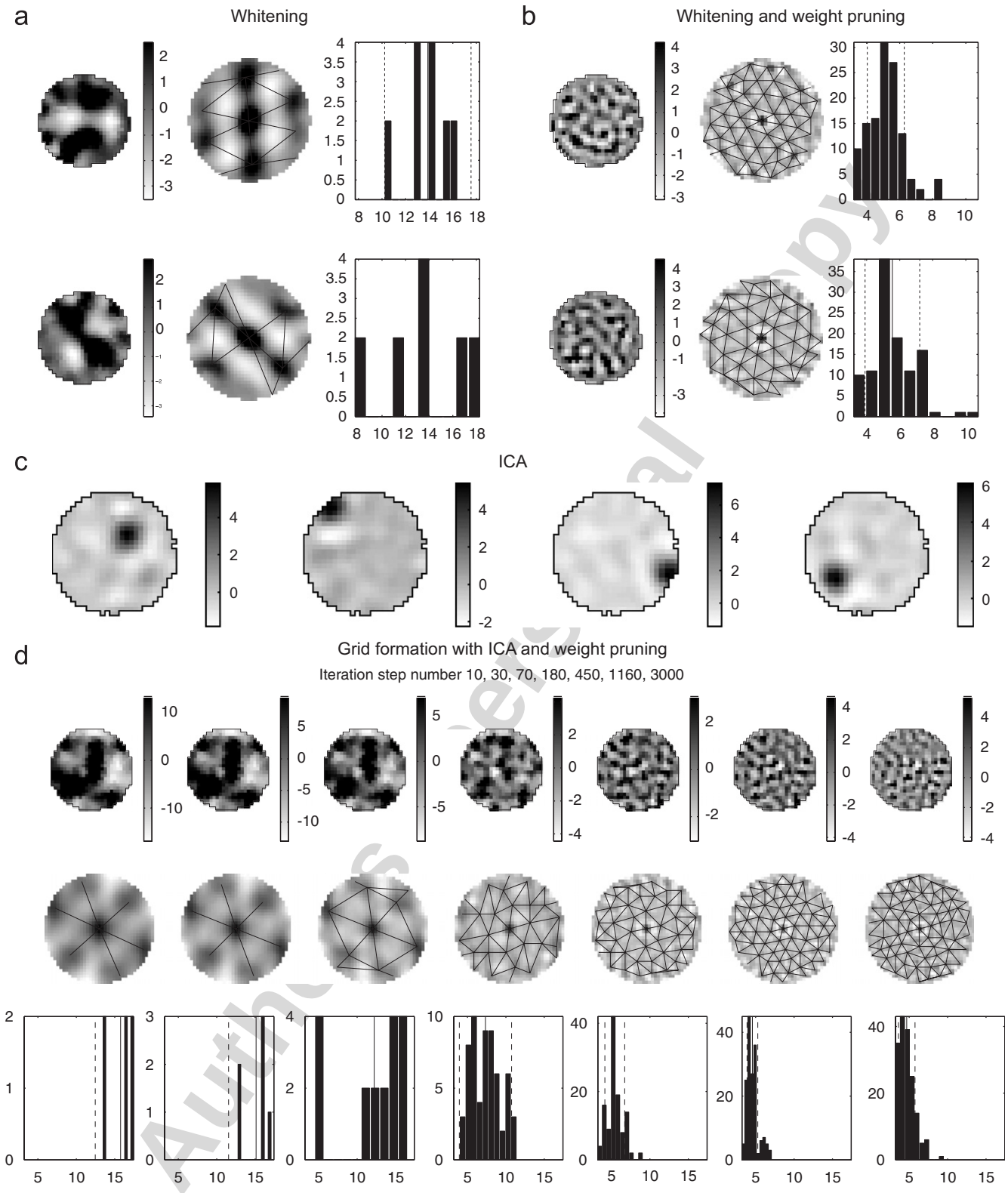

Fig. 2. *Activity maps in circular labyrinth*: The total number of trained neurons (i.e., dim(**y**)) was 30: (a) Activity maps formed by whitening; (b) Activity maps formed by whitening and weight pruning. For (a) and (b) two typical instances are shown. Activity maps with gray coded activity values, correlograms, and the histograms of the grid edges are depicted. (c) Activity maps formed by ICA. The FastICA algorithm was used because it is parameter free. The input for ICA was provided by 300 randomly generated neurons, similar to those shown in Fig. 1(b). (d) Formation after 10, 30, 70, 180, 450, 1160, and 3000 steps made in the labyrinth. Upper row: activity maps with gray coded activity values, middle row: correlograms, lower row: histograms of the grid edges.

pruning. We found that the weight pruning rule (Eq. (1)) diminishes the weights if it acts alone and during this process it forms triangular grids. The weight decreasing property of the anti-Hebbian rule follows from the cost function $J = \frac{1}{2}\sum_{t=t_i}^{t_f} \mathbf{y}_t^{\mathrm{T}}\mathbf{y}_t$, where training starts and finishes at times $t = t_i$ and $t = t_f$, respectively. The negative gradient of cost function J is proportional to the r.h.s. of Eq. (1).

The anti-Hebbian rule penalizes connection weights the most which tend to be active simultaneously with other connections. This is easy to see from the cost function above. A simple thought experiment explains why the remaining active spatial fields will be arranged into a grid of tight packing. Imagine that a number of paper sheets of various shape (equivalent to the input's receptive fields) are dropped on the floor. Each sheet overlaps with other sheets, maybe with multiple ones. Then start to remove sheets, always selecting the sheet which has the biggest overlap with other sheets in total (sum multiple overlaps here). Stop removing the sheets when none of them overlaps. You will get a formation where the sheets has the closest possible distance to each other, which in turn results in a tight-packing formation. To illustrate our findings, the sheets in this example must fulfill some requirements: (1) the circle which is a subset of all sheets should have a size of the same magnitude as the fields itself, otherwise the resulting formation should cover all the available floor space (because we will always find sheets which fit into the holes between sheets); (2) the sheets must have a randomized shape, otherwise special tight formations may emerge. For example, if all sheets are rectangular, a quadratic grid is a tighter packing than the triangular one. Nevertheless, if the number of sheets is limited, a triangular grid may emerge in these cases as well if the sheets are oriented randomly.

The explanation described above is a bit misleading in that sense that anti-Hebbian rule can produce negative weights as well, so we do not have to really remove papers, only mix weights to cancel overlapping areas. However, the receptive fields of the input we used fulfill both requirements identified above. In our experiment, only deep local minima that seem to occur for dense packing of high and low responses can survive.[3]

Note that we had not exploited reliable spatial selectivity of specific input cells in our experiments. It is true that overall spatial selectivity of individual inputs is a requirement, however, it is more important that a huge number of input cells should be present then the stability of their fields. If any of the cells changes its spatial modulation, the anti-Hebb rule will immediately discard its contribution to the grid, and ICA or whitening will raise an other cell to replenish the discarded one and the grid remains stabilized (until there is enough cells to select from).

[3]In rate code models, threshold are used to shift positive and negative responses into the positive region. In our studies, such shifts have been neglected.

Whitening or ICA can counteract the weight decreasing process and ensure that the weights stay finite. We note that (i) in many cases when anti-Hebbian weight pruning was used alone, weights did not disappear, but became stuck in local minima for our invariant sensors. Also (ii) when weight pruning was combined either with ICA or with whitening, the triangular grid-like activity maps kept changing, these changes converged but did not disappear. In spite of the changes, the overall triangular structure remained and was stable (Fig. 2(d)).

Experimental results show that grids are not formed if the HC is lesioned [6]. From the point of view of the superficial layers of the EC, postrhinal information is transferred bottom-up, whereas information from the HC is transferred top-down. In order to save the suggestion of bottom-up information maximization, we have to consider the following constraints. There is no grid without the HC according to the experiments. There is no grid without weight pruning in the model. Neither bottom-up whitening nor bottom-up ICA lead to grids. Bottom-up ICA cannot be the only training process *either with or without* the HC, because it would form place cells, which were not found experimentally in the EC. Thus, whitening is the main component of the bottom-up process and we make the following conjectures:

(1) Bottom-up transformations are trained both by bottom-up and by top-down information.
(2) Bottom-up training corresponds to whitening.
(3) Top-down information is the origin of weight pruning.
(4) Top-down information enhances bottom-up information maximization.

This last suggestion is supported by our finding that weight pruning with ICA produces more robust hexagonal grids than weight pruning with whitening. Another consequence of this model is that place field formation will occur in the HC provided that the HC performs ICA as suggested in [9–11,15].

Our model suggests a mechanism how HC outputs may alter synaptic connections in those cortical networks whose activity gave rise to hippocampal input: top-down effects includes HC driven pruning of bottom-up weights. Top-down effects constrain the pruning process by enhancing bottom-up information maximization. Below, we shall elaborate this conjecture.

4.1. Two-phase computational model of the entorhinal–hippocampal region

Model [10] was derived from a few principles and yielded the following concepts (see also [11,15]). The entorhinal–hippocampal loop works as a comparator that compares input to *reconstructed input*. Reconstructed input is generated by the *hidden representation*. The goal of this hidden representation is to minimize the result of the comparison, the *reconstruction error*. Then the necessity of

optimal information transfer from input to the hidden representation follows. Optimal information transfer—in the model—is enabled by bottom-up ICA. The model assumed additional noise filtering and spatio–temporal pattern completion mechanisms.

Computational tasks of the loop were distributed as follows. Hidden representation is held by the deep layers of the EC. Reconstructed input is generated at EC layer III. Comparison of input and reconstructed input occurs at EC layer II. Bottom-up information maximization is the task of the HC. According to the model, the CA1 subfield of the HC holds the independent components of the error signal. Recurrent network at the internal representation has a *predictive role*, it propagates activities forward in time to minimize the delays of the network [11,15]. The output of the CA1 subfield corrects the internal representation, which, in turn, corrects the reconstruction of the input at EC layers II and III. The reconstructed input is compared to the original input and the iteration goes on. This is the operation of the loop in the theta phase.

In the sharp wave phase [3], activity patterns originate from the CA3 subfield, these patterns are guided by the recurrent collaterals of this subfield replay and generate spike sequences experienced during the theta phase. Sharp waves train long-term memories in the EC and in the neocortex. The EC deep layer to superficial layer connections belong to the long-term memory system according to the model and these connections are trained by the Hebbian Delta-rule.

4.2. Connecting grid formation and the computational model of the EC–HC loop

The two-phase model explains how connections between deep EC and superficial EC layers are trained. This is a falsifying suggestion and it has received experimental support recently: according to [17], long-term potentiation (LTP) was reliably induced in the deep-to-superficial layer projections by burst stimulations that emulated theta or sharp wave patterns. Also, a weak stimulation of deep layers, which induced a small degree of LTP by itself, generated a much larger degree of LTP when paired with a strong stimulation of superficial layers. This is exactly that follows from the model [10,15].

The present model can take this suggestion one step further. The HC plays at least two distinct roles:

(1) The HC supports weight pruning that improves generalization capabilities [8].
(2) The HC may induce or enhance the maximization of bottom-up information transfer. From the point of view of the equations (Eqs. (2) and (3), bottom-up information transfer can be modulated top-down, because in these equations trainingg is directed by output neural activities. Top-down modulation is straightforward in the two-phase model [10,15] by construction (see below).

Thus we can elaborate our conjectures further: The EC–HC loop plays a role in the formation of the afferents of the EC superficial layers through the reconstructed input. This top-down influence is the trick of the loop. According to the constraints of the comparator function, the reconstructed input (at layer III) closely matches the input (at layer II). Thus, if the EC–HC loop is trained properly, then the bottom-up processed input to the loop and the HC processed top-down information are about the same at the superficial layers. In other words, training rules remain unchanged if the components of vector $\mathbf{y}$ in Eqs. (1)–(5) are the result of (i) the bottom-up transformation, or (ii) the feedback from the HC, or both. Thus, different components of Eqs. (1)–(5) may have different origins. The weight pruning effect as well as non-linearities required for information maximization that counteracts weight pruning may be top-down effects. They may originate from feedback from the HC. This conjecture can explain experimental findings.

Our model suggests that the observed stability of grid cells is not a consequence of low-level idiothetic information, rather a side-effect of generalization occurring on a higher level. It requires further effort to prove that generalization occurring at the HC is able to produce stabilized grids across different environments.

The proposed generalization role of the HC does not contradict the emergence of generalized features in the EC. The HC influences EC in a top-down manner, and any generalization discovered in the EC can possibly be the consequence of HC bottom-up transformations. It requires further work to investigate whether the model can produce, for example, 'path equivalent' firings similar to those observed in U-shaped labyrinths [4].

There are recent attractor models in the literature [16,5]. These models—which are not using robotic simulations—produce very precise triangular grids. These triangular grids are superior to ours. We expect that the two models need to be connected. Present attractor models cannot account for the lack of triangular grid formation if the HC is lesioned. On the other hand, precise grid lengths cannot be achieved in the present model, but they can be achieved in attractor models.

5. Conclusions

We searched for simple training rules that can form triangular grids from sensory information. We could develop such grids from invariant 'neural responses'. Training rules that can produce non-vanishing grids, combine weight pruning with either whitening or with independent component analysis. These training rule combinations are minimal in the sense that we were unable to generate triangular grids by less complex learning methods. The training rules produced different grid spacings for different average sizes of the 'blobs' of the invariant neural responses. Non-grid like responses were

formed when inputs contained strong directional information.

In spite of the simplicity of our model, we could connect it to the computational model of the EC–HC region [10]. There are several consequences of this connection. One of them is that triangular grids may not be prerequisites of the formation of place cells in the hippocampus.

Acknowledgments

We are most grateful to Gyuri Buzsáki for his continuous support in our work. Helpful discussions with Trygve Solstad are also acknowledged. We thank Melinda Kiszlinger for her help in the computer runs.

References

[1] F. Attneave, Some informational aspects of visual perception, Psychol. Rev. 61 (1954) 183–193.
[2] H. B. Barlow, Sensory Communication, W. A. Rosenblith ed., MIT Press, Cambridge, MA, 1961, pp. 217–234.
[3] G. Buzsáki, Feed-forward inhibition in the hippocampal formation, Prog. Neurobiol. 22 (1984) 131–153.
[4] L.M. Frank, E.N. Brown, M.A. Wilson, A comparison of the firing properties of putative excitatory and inhibitory neurons from ca1 and the entorhinal cortex, J. Neurophysiol. 86 (2001) 2029–2040.
[5] M.C. Fuhs, D.S. Touretzky, A spin glass model of path integration in rat medial entorhinal cortex, J. Neurosci. 26 (2006) 4266–4276.
[6] M. Fyhn, S. Molden, M.P. Witter, E.I. Moser, M. Moser, Spatial representation in the entorhinal cortex, Science 305 (2004) 1258–1264.
[7] T. Hafting, M. Fyhn, S. Molden, M. Moser, E.I. Moser, Microstructure of a spatial map in the entorhinal cortex, doi:10.1038/nature03721 (2005).
[8] S. Haykin, Neural Networks: A Comprehensive Foundation, Prentice-Hall, NJ, USA, 1999.
[9] A. Lőrincz, Forming independent components via temporal locking of reconstruction architectures: a functional model of the hippocampus, Biol. Cybern. 79 (1998) 263–275.
[10] A. Lőrincz, G. Buzsáki, Two-phase computational model training long–term memories in the entorhinal–hippocampal region, NYAS 911 (2000) 83–111.
[11] A. Lőrincz, B. Szatmáry, G. Szirtes, Mystery of structure and function of sensory processing areas of the neocortex: a resolution, J. Comput. Neurosci. 13 (2002) 187–205.
[12] W.B. Scoville, B. Milner, Loss of recent memory after bilateral hippocampal lesions, J. Neurol. Neurosurg. Psychiatry 20 (1957) 11–21.
[13] L.R. Squire, Declarative and nondeclarative memory: multiple brain systems supporting learning and memory, J. Cog. Neurosci. 4 (1992) 232–243.
[14] L.R. Squire, Memory and the hippocampus: a synthesis of findings with rats, monkeys, and humans, Psychol. Rev. 99 (1992) 195–231.
[15] G. Szirtes, B. Póczos, A. Lőrincz, Neural Kalman-filter, Neurocomputing 65–66 (2005) 349–355.
[16] A. Treves, E. Kropff, A. Biswas, On the triangular grid formation of entorhinal place fields, in: Abstract Viewer/Itinerary Planner, Program No. 198.11., Society for Neuroscience, Washington, DC, 2005, online.
[17] S. Yang, D. Lee, C. Chung, M. Cheong, C. Lee, M. Jung, Long-term synaptic plasticity in deep layer-originated associational projections to superficial layers of rat entorhinal cortex, Neurosci. 127 (2004) 805–812.

Bálint Takács was born in 1976. He obtained his M.Sc. degree in physics in 2000 and in computer science in 2002. He has won the Pro Scientia Award of the National Scientific Students' Associations and is about to finish his Ph.D. studies in Computer Sciences in András Lörincz's group at the Eötvös Loránd University of Sciences, Budapest, Hungary. Currently he is working at Imperial College, London under the supervision of Yiannis Demiris. His main interests include reinforcement learning, probabilistic learning methods, functional modeling of biological neural systems and human–computer interfaces.

András Lőrincz professor, senior researcher. He has been teaching and doing research at the Faculty of Informatics at Eötvös University, Budapest since 1998. His research focuses on distributed intelligent systems and their applications in neurobiological and cognitive modeling, as well as medicine. He directs a multidisciplinary team of mathematicians, programmers, computer scientists and physicists. He has acted as the PI of several successful international projects in collaboration with Panasonic, Honda Future Technology Research and the Information Directorate of the US Air Force in the fields of hardware–software co-synthesis, image processing and human–computer collaboration.

He graduated in physics at the Eötvös Loránd University in 1975 where he received his Ph.D. in 1978 and his C.Sc. in 1986 in experimental and theoretical solid-state physics and chemical physics, respectively. He conducted research and taught quantum control, photoacoustics and artificial intelligence at the Hungarian Academy of Sciences, University of Chicago, Brown University, Princeton University, the Illinois Institute of Technology and ETH Zurich. He authored over 200 peer reviewed scientific publications.

He has received the Széchenyi Professor Award, Master Professor Award and the Széchenyi István Award in 2000, 2001, and 2004, respectively. Four of his students won the prestigious Pro Scientia Gold Medal in the field of information science over the last 4 years. In 2004, he was awarded the Kalmár Prize of the John von Neumann Computer Society of Hungary. He has become an elected Fellow of the European Coordinating Committee for Artificial Intelligence in 2006.